frontiers | Frontiers in Energy Research

REVIEW
published: 20 June 2022
doi: 10.3389/fenrg.2022.862551

Review: High-Entropy Materials for Lithium-Ion Battery Electrodes

James W. Sturman[1,2], *Elena A. Baranova*[2] *and Yaser Abu-Lebdeh*[1]*

[1]*Energy, Mining and Environment Research Centre, National Research Council of Canada, Ottawa, ON, Canada,* [2]*Department of Chemical and Biological Engineering, Centre for Catalysis Research and Innovation (CCRI), University of Ottawa, Ottawa, ON, Canada*

The lithium-ion battery is a type of rechargeable power source with applications in portable electronics and electric vehicles. There is a thrust in the industry to increase the capacity of electrode materials and hence the energy density of the battery. The high-entropy (HE) concept is one strategy that may allow for the compositional variability needed to design new materials for next-generation batteries. Inspired by HE-alloys, HE-oxides are an emerging class of multicomponent ceramics with promising electrochemical properties. This review will focus on the application of these materials to the development of new battery electrodes with insight into the materials' structure/property relationship and battery performance. We highlight recent results on HE-oxides for the cathode and anode. In addition, we discuss some emerging results on HE-solid electrolytes and HE-alloy anodes.

Keywords: energy storage, lithium-ion battery, high-entropy, alloys, ceramic oxides, electrode materials

OPEN ACCESS

Edited by:
Qingsong Wang,
University of Bayreuth, Germany

Reviewed by:
Qiongqiong Lu,
Leibniz Institute for Solid State and Materials Research Dresden (IFW Dresden), Germany
Junchao Zheng,
Central South University, China

***Correspondence:**
Yaser Abu-Lebdeh
Yaser.Abu-Lebdeh@nrc-cnrc.gc.ca

Specialty section:
This article was submitted to Electrochemical Energy Conversion and Storage, a section of the journal Frontiers in Energy Research

Received: *26 January 2022*
Accepted: *23 May 2022*
Published: *20 June 2022*

Citation:
Sturman JW, Baranova EA and Abu-Lebdeh Y (2022) Review: High-Entropy Materials for Lithium-Ion Battery Electrodes. Front. Energy Res. 10:862551. doi: 10.3389/fenrg.2022.862551

INTRODUCTION AND WORKING PRINCIPLES

Multicomponent or high-entropy alloys (HEA) differ from traditional alloys in that they consist of multiple principal elements. HEAs were introduced in 2004 independently by authors Cantor and Yeh (Cantor et al., 2004; Yeh et al., 2004). Since then, high-entropy alloys have primarily been studied in the context of metallurgy, where they are known to provide desirable properties such as high strength and corrosion resistance (Pickering and Jones, 2016; Zhang, 2019). The role entropy plays in the phase stability of these compounds can be understood in terms of the Gibbs free energy of mixing (ΔG_{mix}) (Rost et al., 2015; Widom, 2018; Akrami et al., 2021; Xiang H. et al., 2021; Chen et al., 2021; Fu et al., 2021; Ma et al., 2021):

$$\Delta G_{mix} = \Delta H_{mix} - T\Delta S_{mix} \quad (1)$$

where ΔH_{mix} is the mixing enthalpy, ΔS_{mix} is the mixing entropy, and T is the absolute temperature. If the $T\Delta S_{mix}$ term dominates the enthalpy term (ΔH_{mix}), the overall ΔG_{mix} becomes negative and entropy stabilization has been established. The mixing entropy (ΔS_{mix}) includes many entropic terms, however the configurational entropy (ΔS_{conf}) is usually the dominant contribution (Chen et al., 2021). Configurational entropy for an ideal solid solution is proportional to the number of components *n*: (Chen et al., 2021; Ma et al., 2021)

$$\Delta S_{conf} = -R\sum_{i=1}^{n} x_i ln x_i \quad (2)$$

where *R* is the ideal gas constant and x_i is the component mole fraction. When all components are present in equimolar proportion, the configurational entropy reaches its maximum and **Eq. (2)** simplifies to the equation below: (Chen et al., 2021; Ma et al., 2021)

$$\Delta S_{conf} = Rln(n) \quad (3)$$

There are two formal definitions of high-entropy alloys. First, the compositional based definition states that the alloy must contain at least five elements, with each having an atomic percentage between 5% and 35% (Zhang, 2019; Ma et al., 2021). This definition has often been used in physical metallurgy where it is common to dope alloys with small quantities of elements. Second, the entropy-based definition states that an alloy is high-entropy when ΔS_{conf} is greater than 1.5R (Zhang, 2019; Ma et al., 2021). This criterion is satisfied for a solid solution with five equimolar components, where the ΔS_{conf} of **Eq. (3)** simplifies to 1.61R.

Four "core effects" are believed to be responsible for the unique properties of high-entropy materials: the aforementioned entropy stabilizing effect, lattice distortion, sluggish diffusion, and the so-called cocktail effect (Yeh, 2015; Pickering and Jones, 2016). Lattice distortion results from the different atomic sizes of the constituent elements. This can provide benefits like increased alloy strength or allow for the storage of hydrogen into interstitial sites (Pickering and Jones, 2016; Ma et al., 2021). Sluggish diffusion refers to the low diffusion and phase transformation rates from the fluctuations of lattice potential energy (Yeh, 2015). Finally, the "cocktail effect" is the synergistic effect believed to result from the interplay between composition, structure, and microstructure (Yeh, 2015; Pickering and Jones, 2016). However, these "core effects" are not necessarily unique to high-entropy materials (HEM), and some authors have disputed their contribution to material properties (Pickering and Jones, 2016). HEMs have an additional economic benefit since they are often composed of inexpensive metals, which reduces reliance on any single element (e.g., Co.).

High-entropy oxides (HEO) are a newer class of HE material with numerous applications in energy storage. Like HEAs, entropy-based definitions have been proposed for HEOs, where the configurational entropy from both cations and anions is considered (Sarkar et al., 2018a; Sarkar et al., 2020b). Typically, the O^{2-} anion entropy contribution is zero, but the presence of oxygen vacancies or other anions (e.g., F^{-}) can contribute to the system's entropy (Sarkar et al., 2020b). In practice, it is difficult to determine whether a multicomponent oxide is truly entropy stabilized. The term "entropy-stabilized oxides" should be reserved for materials with a proven entropy-driven reversible phase transformation (Sarkar et al., 2020b). As a result, the term "high-entropy" is more often employed to describe an oxide system containing five or more equimolar cations.

In 2015, Rost et al. showed that the (NiCuZnMgCo)O HEO could be stabilized into a single-phase rock-salt structure (Rost et al., 2015). This was of interest to battery researchers as it allowed for the possibility of high-entropy electrodes, which are often oxide ceramics. The authors were able to show a reversible transformation from multi-phase to single-phase by varying calcination temperature. The transition was an endothermic process ($\Delta H>0$); hence the system was entropy stabilized because the $T\Delta S$ term must be large enough to overcome the positive enthalpy and render the Gibbs free energy negative. The removal of any one of the five components destabilized the solid solution, as seen in the X-ray diffraction (XRD) data of **Figure 1A**. This highlights the importance of five cations in entropy stabilized oxides. In addition, phase diagrams in **Figure 1B** confirm that the minimum transition temperature required for the formation of a single-phase occurs at maximum configurational entropy (Rost et al., 2015).

Today, the high-entropy concept has been applied to alloys, oxides, carbides, nitrides, borides, hydrides, sulfides, among others (Fu et al., 2021). Over 50 high-entropy oxides are known and take on a variety of crystal structures including rock-salt, perovskite, fluorite, spinel, and layered (**Figure 1C**) (Sarkar et al., 2020b; Akrami et al., 2021). As seen in **Figure 1D**, publications on the topic have accelerated over the past few years, including a number of reviews (Widom, 2018; Vaidya, Muralikrishna and Murty, 2019; Sarkar et al., 2020b; Akrami et al., 2021; Amiri and Shahbazian-Yassar, 2021; Chen et al., 2021; Fu et al., 2021; Lin et al., 2021; Ma et al., 2021; Wang Q. et al., 2021). For energy storage, HEOs have shown promising results in the fields of batteries, supercapacitors, electrochemical catalysis, hydrogen storage, hydrogen evolution reaction, oxygen evolution reaction, carbon dioxide conversion, and oxidation reactions involving methanol, ethanol, or formic acid (Sarkar et al., 2017b; Sarkar, et al., 2018a; Wang, et al., 2019a; Sarkar et al., 2019; Fu et al., 2021; Ma et al., 2021; Sturman et al., 2021; Sun et al., 2022). In battery research, HEMs are often used as electrode materials for Li-ion batteries, but they have also been used in solid electrolytes, Li-Sulfur and Na-ion batteries, as well as MXenes (Bérardan et al., 2016; Zhao et al., 2020; Akrami et al., 2021; Fu et al., 2021; Nemani et al., 2021; Xu et al., 2021; Yang et al., 2021; Etman, Zhou and Rosen, 2022). Consult **Table 1** for a list of recent publications on high-entropy materials for battery applications. In this review, we have summarized the recent research on HEMs with an emphasis on their use as anodes and cathodes for Li-ion batteries. In addition, we discuss common synthesis methods, characterization techniques, electrochemical performance, and proposed lithiation and failure mechanisms.

MATERIAL PREPARATION AND CHARACTERIZATION

Synthesis and Material Discovery

The most common methods of HEA synthesis include arc melting and mechanical alloying (Vaidya, Muralikrishna and Murty, 2019; Zhang, 2019). Mechanical alloying is widely used in the production of nanocrystalline HEAs. Preparation involves ball-milling of stoichiometric amounts of the metal powders followed by sintering (Vaidya, Muralikrishna and Murty, 2019). The cooling rate is important to the formation of a single-phase, and quenching can be used to cool the material after heating. Moreover, de-alloying (where one element is selectively leached) can be used to create nano-porous HEAs with high catalytic activity (Fu et al., 2021).

In contrast, the synthesis of HEOs often requires high temperature methods like solid-state sintering or spray pyrolysis (Sarkar et al., 2020b; Akrami et al., 2021; Fu et al.,

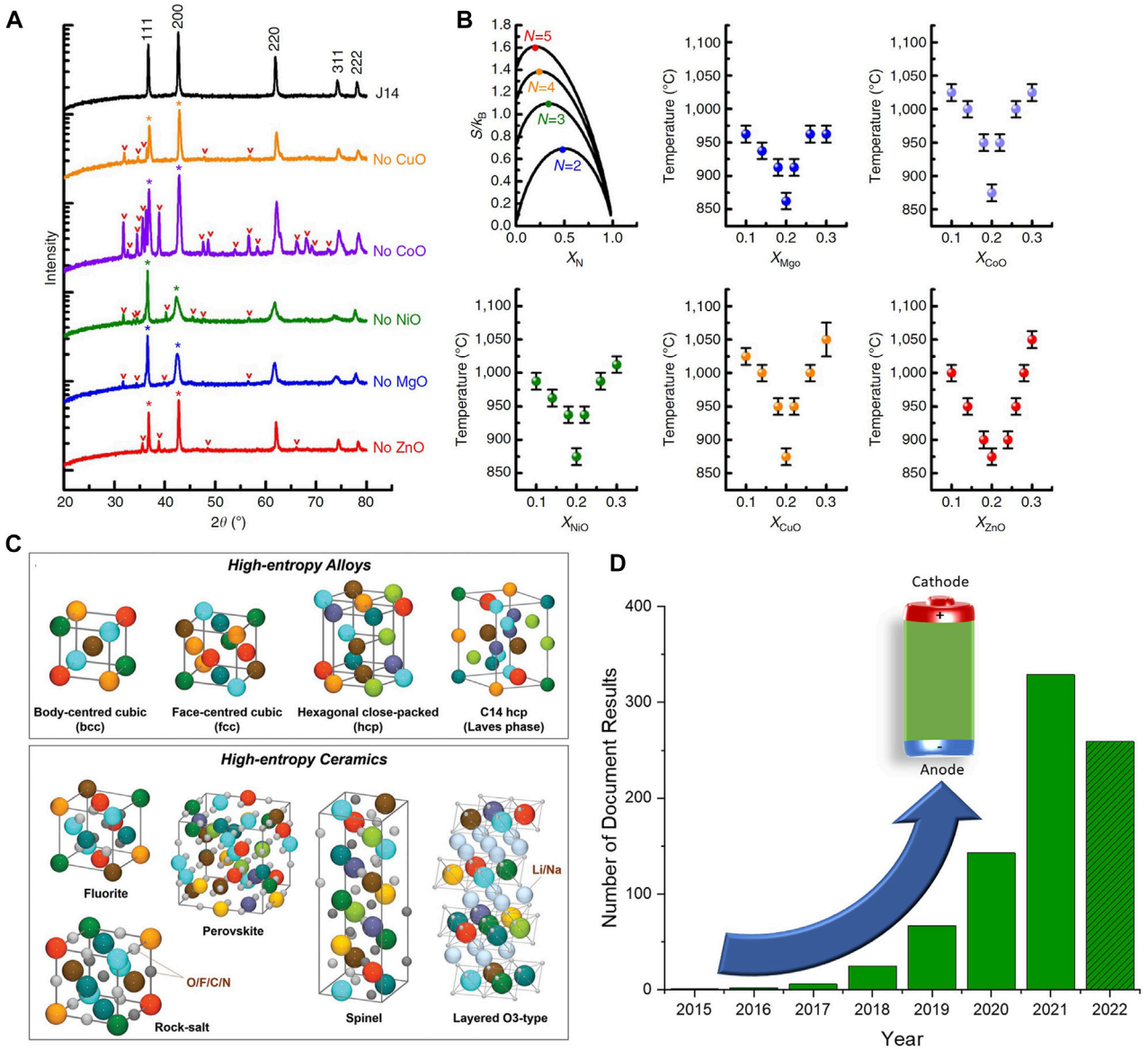

FIGURE 1 | (A) XRD of multicomponent oxides **(B)** configurational entropy and phase diagrams of HEO elements (Rost et al., 2015). **(C)** common crystal structures for HEAs and HEOs (Ma et al., 2021). Reproduced under the terms of the CC BY license. **(D)** Rapid growth in publications on high-entropy materials for energy storage. Data was gathered from Scopus by searching for high-entropy oxides, anodes, or cathodes, and limiting the search to material science and energy. Please note data from 2022 includes only Jan-Apr.

2021). Other methods include sol-gel combustion, coprecipitation, sonochemical, carbothermal shock, or sputtering deposition for the synthesis of thin films (Fu et al., 2021). With solid state methods, metal oxides are ball-milled, pelletized, and sintered for multiple hours. In contrast, spray pyrolysis is desirable as it has a shorter residence time at elevated temperatures. It can produce nanocrystalline powders by passing an aerosol of metal precursors through a flame or reactor to induce rapid decomposition and structural transformation (Sarkar et al., 2020b). Sarkar et al. showed that nanocrystalline HEOs can be prepared by nebulized spray pyrolysis (NSP), flame spray pyrolysis (FSP), and reverse co-precipitation (Sarkar et al., 2017b). NSP was preferred as it was able to directly synthesize nanocrystalline single-phase rock-salt structures, whereas the other techniques required additional thermal treatments. The authors also confirmed the importance of a high configurational entropy when preparing these samples. A 4-cation (medium entropy) sample required a higher temperature to achieve single-phase. Other studies have also reported difficulty in preparing single-phase medium entropy oxides (Sarkar, et al., 2018a).

Green synthesis methods for HEOs are increasingly the focus of publications. Kheradmandfard et al. used a microwave-assisted method to produce (MgCuNiCoZn)O *nano*particles (ave. size

TABLE 1 | Select Publications on High-Entropy Oxides for Li-ion Batteries.

Primary Composition	First Author and Year	Synthesis Method	Structure	Battery Performance	References
(MgNiCoCuZn)O	Rost, 2015	Solid State	Rock-salt	Fundamental characterization	Rost et al. (2015)
(CeLaPrSmY)O	Djenadic, 2017	Nebulized spray pyrolysis (NSP)	CaF_2-type	Fundamental characterization on rare earth HEO	Djenadic et al. (2017)
(CoCuMgNiZn)O	Sarkar, 2017	reverse co-precipitation (RCP) (NSP) flame spray pyrolysis (FSP)	Rock-salt	Investigation of synthesis methods	Sarkar et al. (2017b)
$(CeLaPrSmY)O_{2-\delta}$	Sarkar, 2017	NSP	Fluorite type	Fundamental characterization	Sarkar et al. (2017a)
$(Co_{0.2}Cu_{0.2}Mg_{0.2}Ni_{0.2}Zn_{0.2})O$	Sarkar, 2018	NSP	Rock-salt	Anode. 500 mAh/g at 0.1 A/g	Sarkar et al. (2018a)
$(Gd_{0.2}La_{0.2}Nd_{0.2}Sm_{0.2}Y_{0.2})(Co_{0.2}Cr_{0.2}Fe_{0.2}Mn_{0.2}Ni_{0.2})O_3$	Sarkar, 2018	NSP	Perovskite	Fundamental characterization	Sarkar et al. (2018b)
$(Mg_{0.2}Co_{0.2}Ni_{0.2}Zn_{0.2}Li_{0.2})O$	Anik, 2019	Solid State	Rock-salt	Anode. 720 mAh/g after 10 cycles at 0.1 A/g	Anik and Lokcu, (2019)
$(Mg_{0.2}Co_{0.2}Ni_{0.2}Cu_{0.2}Zn_{0.2}O)$	Qiu, 2019	Solid State	Rock-salt	Anode. 920 mAh/g after 300 cycles at 0.1 A/g	Qiu *et al.* (2019)
$(Li_x(Co_{0.2}Cu_{0.2}Mg_{0.2}Ni_{0.2}Zn_{0.2})OF_x)$	Wang, 2019	Coprecipitation and ball milling	Rock-salt oxyfluoride	Cathode. 90 mAh/g after 100 cycles at C/10	Wang et al. (2019b)
$Gd(Co_{0.2}Cr_{0.2}Fe_{0.2}Mn_{0.2}Ni_{0.2})O_3$	Witte, 2019	NSP	Perovskite	Investigation of magnetic properties	Witte et al. (2019)
$(Co_{0.2}Cu_{0.2}Mg_{0.2}Ni_{0.2}Zn_{0.2})O$ Rock-salt	Wang, 2019	NSP		Anode in full cell. 300 mAh/g after 50 cycles at 0.12 A/g	Wang et al. (2019a)
Multiple HEOs	Chellali, 2019	NSP	Rock-salt, fluorite, and perovskite	Fundamental characterization with atom probe tomography	Chellali et al. (2019)
$(Ce_{0.2}La_{0.2}Pr_{0.2}Sm_{0.2}Y_{0.2})O_{2-\delta}$	Cheng, 2019	NSP	CaF_2-type	High-pressure characterization	Cheng et al. (2019)
$(Mg_{0.2}Co_{0.2}Ni_{0.2}Cu_{0.2}Zn_{0.2})O$	Chen, 2019	Solid State	Rock-salt	Studied pseudocapacitive contribution. Anode. 900 mAh/g after 150 cycles at 0.2 A/g	Chen et al. (2019)
$(FeCoNiCrMn)_3O_4$	Wang, 2020	Solid State	Spinel	Anode. 402 mAh/g after 300 cycles at 0.5 A/g	(D. Wang et al., 2020a)
$(Mg_{0.2}Ti_{0.2}Zn_{0.2}Cu_{0.2}Fe_{0.2})_3O_4$	Chen, 2020	Solid State	Spinel	Anode. 504 mAh/g after 300 cycles at 0.1 A/g	Chen et al. (2020)
Non-equimolar cations with Cr, Mn, Fe, Co., and Ni	Nguyen, 2020	Hydrothermal method	Spinel	Anode. 500 mAh/g at 2 A/g	Nguyen et al. (2020)
$(MgCoNiZn)_{0.65}Li_{0.35}O$	Lökçü, 2020	Solid State	Rock-salt	Anode. 610 mAh/g after 130 cycles at 1 A/g	Lökçü et al. (2020)
$[(Bi,Na)_{1/5}(La,Li)_{1/5}(Ce,K)_{1/5}Ca_{1/5}Sr_{1/5}]TiO_3$	Yan, 2020	Solid State	Perovskite	Anode. 85 mAh/g after 50 cycles at 0.1 A/g	Yan *et al.* (2020)
$Li_x(NiFeMnCrCo)_yO_z$	Wang, 2020	NSP	Spinel and Rock-salts	Investigation of spinel to rock-salt transformation	(J. Wang, et al., 2020c)
$LiNa(NiCoMnAlFe)_1O_2$	Wang, 2020	NSP	Layered	Cathode. 75 mAh/g after 15 cycles at C/10	(J. Wang, et al., 2020b)
$(Ce_{0.2}La_{0.2}Pr_{0.2}Sm_{0.2}Y_{0.2})O_{2-\delta}$	Sarkar, 2020	Reverse coprecipitation	Fluorite	Fundamental characterization	Sarkar et al. (2020a)
$Mg_{0.2}Co_{0.2}Ni_{0.2}Cu_{0.2}Zn_{0.2}O$	Ghigna, 2020	Solid State	Rock-salt	Anode. 600 mAh/g at 0.1 C Mechanism investigation with operando XAS	Ghigna et al. (2020)
$(Gd_{0.2}La_{0.2}Nd_{0.2}Sm_{0.2}Y_{0.2})CoO_3$	Witte, 2020	NSP	Perovskite	Investigation of magnetic properties	Witte et al. (2020)
$(Mg_{0.2}Co_{0.2}Ni_{0.2}Cu_{0.2}Zn_{0.2})O$	Tavani, 2020	Solid State	Rock-salt	Mechanism investigation	Tavani et al. (2020)
$(Co_{0.2}Cu_{0.2}Mg_{0.2}Ni_{0.2}Zn_{0.2})O$ and $Li(Co_{0.2}Cu_{0.2}Mg_{0.2}Ni_{0.2}Zn_{0.2})OF$	Breitung, 2020	NSP and solid state	Rock-salt	Investigation of gassing behaviour	Breitung et al. (2020)
$Li_{1.3}Mn^{2+}_{0.1}Co^{2+}_{0.1}Mn^{3+}_{0.1}Cr^{3+}_{0.1}Ti_{0.1}Nb_{0.2}O_{1.7}F_{0.3}$	Lun, 2021	Solid State	Disordered Rock-salts	Cathode. Initially 307 mAh/g at a rate of 20 mA/g	Lun et al. (2021)
(MgCuNiCoZn)O	Kheradmandfard, 2021	Microwave	Rock-salt	Anode. 325 mAh/g after 1000 cycles at 1 A/g	Kheradmandfard et al. (2021)
$(CrMnFeCoNi)_3O_4$	Huang, 2021	Hydrothermal and sintering	Spinel	Atomic-scale investigation of mechanism	Huang et al. (2021)
$(Al_{0.2}CoCrFeMnNi)_{0.58}O_{4-\delta}$	Xiang, 2021	Solution combustion	Spinel	Anode. 554 mAh/g after 500 cycles at 0.2 A/g	(Hou-zheng Xiang et al., 2021b)

(Continued on following page)

TABLE 1 | (*Continued*) Select Publications on High-Entropy Oxides for Li-ion Batteries.

Primary Composition	First Author and Year	Synthesis Method	Structure	Battery Performance	References
$(Co_{0.2}Cu_{0.2}Mg_{0.2}Ni_{0.2}Zn_{0.2})O$	Schweidler, 2021	NSP	Rock-salt	Acoustic emission investigation of mechanism	Schweidler et al. (2021)
$(Co_{0.2}Cr_{0.2}Fe_{0.2}Mn_{0.2}Ni_{0.2})_3O_4$	Zhao, 2021	Solution combustion	Spinel	Anode. 980 mAh/g after 50 cycles at 0.1 A/g	Zhao et al. (2021)
$Li(Ni_{0.2}Co_{0.2}Mn_{0.2}Ti_{0.2}Fe_{0.2})O_2$	Sturman, 2021	Sol-gel	Layered	Cathode. 85 mAh/g after 50 cycles at C/10	Sturman et al. (2021)
$(CoCuMgNiZn)_{0.8}Li_{0.2}O$	Moździerz, 2021	Solid State	Rock-salt	Fundamental characterization	Moździerz et al. (2021)
$(FeNiCrMnZn)_3O_4$	Xiao, 2021	Solid State	Spinel	Anode. 386 mAh/g after 185 cycles at 0.5 A/g	Xiao et al. (2021)
$(FeCoNiCrMnXLi)_3O_4$ (X = Cu, Mg, Zn)	Duan, 2021	Solid State	Spinel	Anode. 522 mAh/g after 100 cycles at 0.5 A/g	Duan et al. (2021)
(MgCoNiCuZn)O	Wang, 2021	Solid State	Rock-salt	Anode. 550 mAh/g after 100 cycles at 0.1 A/g	(S. Y. Wang et al., 2021b)
Co-free $(CrMnFeNiCu)_3O_4$	Nguyen, 2022	Hydrothermal	Spinel	Anode. 755 mAh/g at 50 mA/g	Nguyen et al. (2022)
$(Mg_{0.2}Co_{0.2}Ni_{0.2}Cu_{0.2}Zn_{0.2})O$	Guo, 2022	Solid State	Rock-salt	Anode. 950 mAh/g after 200 cycles at 0.1 A/g	Guo et al. (2022)
$(MnFeCoNiCuZn)_3O_{4-x}$	Dong, 2022	Rapid heating	Spinel	Anode. 600 mAh/g at 130 mA/g	Dong et al. (2022)
$(CoNiZnXMnLi)_3O_4$ (X = Fe, Cr)	Tian, 2022	Solid State	Spinel	Anode. 260 mAh/g after 100 cycles at 500 mA/g	Tian et al. (2022)
$LiCr_{1/6}Mn_{1/6}Fe_{1/6}Co_{1/6}Ni_{1/6}Cu_{1/6}O_2$	Wang, 2022	Pulsed laser deposition	Layered	Cathode. 40 mAh/g at 5 $\mu A/cm^2$	(K. Wang et al., 2022a)
$Ti_{1.1}V_{0.7}Cr_xNb_{1.0}Ta_{0.6}C_3T_z$	Etman, 2022	Solid State and solution based	MXene	Anode. 40 mAh/g after 1000 cycles at 1 A/g	Etman, Zhou and Rosen, (2022)

Rock-salt: Fm-3m Spinel: Fd-3m Layered: R-3m

44 nm) from nitrate metal precursors (Kheradmandfard et al., 2021). The solution was microwaved for only 3 min and did not require any additional high-temperature sintering. Alternatively, high-entropy oxide *micro*particles of uniform size distribution can be prepared by Joule heating within ~15s (Dong et al., 2022). Surface modifications to rock-salt HEOs have been shown to enhance electrochemical performance. Guo et al. studied graphene modifications to the rock-salt $(Mg_{0.2}Co_{0.2}Ni_{0.2}Cu_{0.2}Zn_{0.2})O$ (Guo et al., 2022). The material was covered with graphene (denoted HEO@G) and increased electrical conductivity and Li-ion diffusion. In addition, they quantified the pseudocapacitive contribution to the capacity.

The importance of composition and temperature has been described for high-entropy perovskites. Sarkar et al. studied several perovskites, including the 10-cation $((Gd_{0.2}La_{0.2}Nd_{0.2}Sm_{0.2}Y_{0.2})(Co_{0.2}Cr_{0.2}Fe_{0.2}Mn_{0.2}Ni_{0.2})O_3)$ (Sarkar, et al., 2018b). They observed single-phase perovskites for 6 out of 11 different samples. The 10-cation sample was phase pure, but other heptanary samples were multiphase. Thus, for certain compositions, the net enthalpic contribution may overcome the high configurational entropy, preventing entropy stabilization. For example, the transition of ZnO (wurtzite) to ZnO (rock-salt) is known to incur a large enthalpic penalty (Rost et al., 2015). Sometimes a higher temperature is sufficient to favour an entropy-driven transformation. This was shown to be true for $(Gd_{0.2}La_{0.2}Nd_{0.2}Sm_{0.2}Y_{0.2})MnO_3$, where a multiphase to single-phase transition occurred upon further heating (Sarkar, et al., 2018b).

In addition to the synthesis procedure, researchers must consider the role individual elements and oxygen vacancies play in the properties of HEOs. Djenadic et al. synthesized HEOs with rare earth elements (CeLaPrSmY)O, among others (Djenadic et al., 2017). They reported that a single-phase compound was not possible without Ce. This highlights the importance of a single element even in the presence of a high configurational entropy. Ce and Zr cations are also necessary to the formation of certain fluorite HEOs (Sarkar et al., 2020b). Sarkar et al. also synthesized and characterized various HEOs with rare earth elements. The materials were shown to have a high level of oxygen vacancies and a narrow band gap (Sarkar, et al., 2017a). The concentration of oxygen vacancies is also known to play a role in the ionic conductivity of high-entropy solid electrolytes (Bérardan et al., 2016).

As researchers identify the complex material-property-performance relationship of HEMs, the true scale of possible material candidates will become apparent. Material discovery has traditionally been guided by a combination of trial and error and systematic exploration (e.g., optimizing calcination temperature of a high-entropy oxide) (Q. Wang et al., 2021a). These approaches are suitable while a field is in its infancy, and they are sure to continue to advance our understanding through the mode of incremental improvement. This is seen, for example, in

the growing body of research on high-entropy oxide spinels. Nevertheless, there is still much work to be done before high-entropy materials can replace traditional Li-ion battery electrodes. It is still unclear to what extent the electrochemical properties of HEMs are governed by element selection, the "cocktail effect", entropy-stabilization, particle size and morphology, etc. In order to accelerate the Technology Readiness Level (TRL) of HEMs, researchers have increasingly relied on computation-driven approaches for material discovery (Q. Wang et al., 2021a). In particular, density functional theory (DFT) and machine learning can help narrow the vast design space of candidates with desirable properties, as will be seen in the work by Lun et al. In addition, high-throughput methods provide the experimental feedback needed to validate these computational methods and complete the material design cycle.

Characterization

Physical characterization methods are necessary to confirm the material's morphology, crystal structure, and composition (Rost et al., 2015; Ma et al., 2021). It is often desired to form a single-phase compound with a defined space group (such as Fd-3m for spinel). X-ray Diffraction (XRD) and Rietveld refinement can be used to determine the crystal structure and space group of the material, as well as reveal the presence of undesired impurity phases. Operando XRD may be used to observe changes in the crystal structure during battery cycling. This can provide information regarding the stability and lithiation mechanism of the material. X-ray Photoelectron Spectroscopy (XPS) is often used to determine the oxidation state of the metal cations or identify oxygen vacancies. This can provide insight into the mechanisms at play before and after lithiation. Scanning Electron Microscopy (SEM) and Transmission Electron Microscopy (TEM) are used to observe morphology. High-Resolution TEM (HR-TEM) is more appropriate in the case of nanoparticles or to verify the d-spacing associated with a particular lattice plane of the structure. Energy-Dispersive X-ray Spectroscopy (EDX) is often used in conjunction with microscopy to quantify the homogeneous distribution of the elements in the sample. More precise quantification of elemental composition can be done with Inductively Coupled Plasma-Optical Emission Spectrometry (ICP-OES). This is particularly important in the synthesis of cathode materials, as there is concern of lithium evaporation at elevated temperatures (>800°C). As a result, many authors include 5–10% excess lithium in their samples prior to calcination.

Electrochemical characterization involves the testing of materials in batteries. Initial testing is usually done in half-cell (vs Li metal) coin-type batteries (such as CR 2032). It is increasingly common to study the material in full cells, which can also be prepared as large-scale pouch cells. A battery electrode is made by first applying a thin film of active material to a current collector. This is usually done by tape casting where the active material powder is combined with a conductive additive (usually carbon), a suitable binder, and mixed with a solvent (usually N-methyl pyrrolidone) to form a slurry. Typically, the binder is polyvinylidene fluoride (PVDF) because of its well-known electrochemical stability. However, polytetrafluoroethylene (PTFE) has been used for certain disordered rock-salts (Lun et al., 2021). The slurry is applied as a thin film to a metal current collector that is subsequently dried and cut into electrodes. Initial electrochemical testing can involve Cyclic Voltammetry (CV) in a defined potential range to identify redox processes. Electrochemical Impedance Spectroscopy (EIS) may also be used to study the resistance of the material before and after cycling. Battery cycling is used to study capacity (energy density) and capacity retention (lifetime), which are the most relevant metrics of performance for practical applications.

HIGH-ENTROPY ANODES

Oxide Ceramics

Graphite has traditionally been used as an anode material in Li-ion batteries. Its intercalation mechanism makes it very stable, but it suffers from a low inherent capacity of 372 mAh/g (Nitta et al., 2015). HEOs for batteries have been used as anode materials owing to their ability to host lithium ions *via* a conversion-type reaction. These materials typically have a capacity much greater than graphite, but they have poor cycle stability. The first cycle coulombic efficiency (CE) is typically less than 90% and is as low as 50% in some cases (Wang et al., 2019b). Many HEOs have the property of increasing capacity with extended cycling. The behaviour is also known to occur with older conversion-type materials such as CoO and $ZnMn_2O_4$. It is generally attributed to reversible lithium storage within a polymeric layer that forms at the electrode surface (Duncan, Courtel and Abu-Lebdeh, 2015). Other explanations include the gradual penetration of the electrolyte into inner oxide pores and structural changes during cycling (Sarkar, et al., 2018a; Qiu et al., 2019; Yan et al., 2020).

One of the most widely studied HEOs for battery applications is the $(Co_{0.2}Cu_{0.2}Mg_{0.2}Ni_{0.2}Zn_{0.2})O$ rock-salt. In 2018, Sarkar et al. synthesized this compound with NSP and used it as an anode that was shown to have a capacity around 500 mAh/g at a current of 0.1 A/g, as seen in **Figures 2A,B** (Sarkar, et al., 2018a). They also tested medium-entropy derivatives of the high-entropy parent structure, but all had a more rapid capacity decay compared to the HEO (**Figure 2B**). Later, the same group successfully used the $(Co_{0.2}Cu_{0.2}Mg_{0.2}Ni_{0.2}Zn_{0.2})O$ HEO as an anode material in a full cell with NMC ($LiNi_{1/3}Mn_{1/3}Co_{1/3}O_2$) as a cathode (Wang et al., 2019a). Despite a low first cycle CE, the anode maintained a capacity of 300 mAh/g after 50 cycles. In addition, the material was used in pouch cells and delivered a capacity of 2.5 mAh. This anode suffered from a large first-cycle irreversible capacity as the initial coulombic efficiency was around 50%. An improvement in the cycling of their full cell was achieved with the pre-lithiation of the anode.

Nanosized $Mg_{0.2}Co_{0.2}Ni_{0.2}Cu_{0.2}Zn_{0.2}O$ rock-salt was synthesized by Qiu et al. (Qiu et al., 2019). It was used as an anode and was compared with the baseline Co_3O_4. The HEO had a first cycle discharge capacity of 1585 mAh/g, compared to 1160 mAh/g for Co_3O_4. In addition, it retained a stable

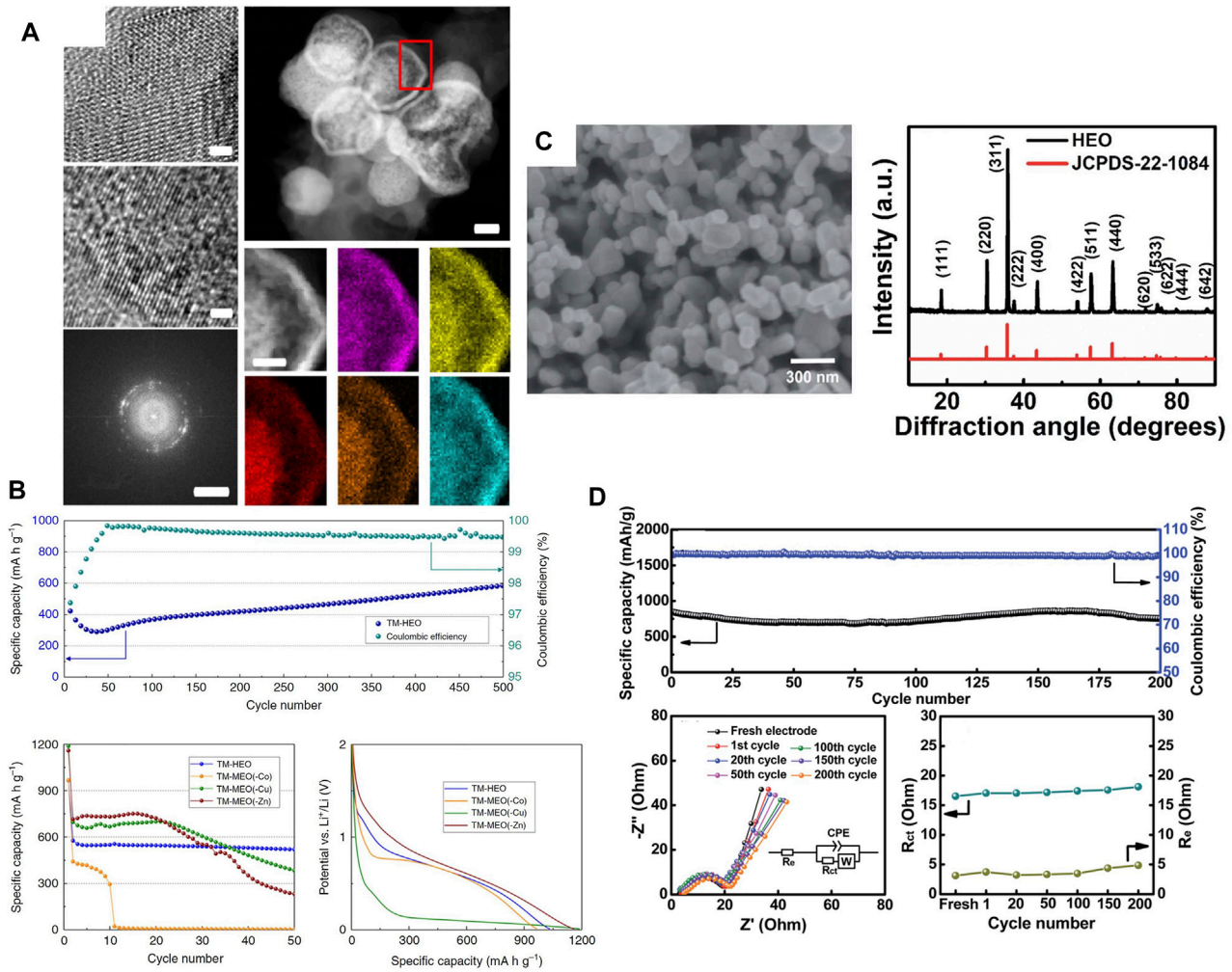

FIGURE 2 | (A) HR-TEM and EDX characterization of rock-salt HEO and **(B)** cycling performance and voltage profiles of high-entropy and medium-entropy oxide anodes (Sarkar, et al., 2018a). **(C)** SEM and XRD characterization and **(D)** cycling performance and impedance of spinel HEO anode (Nguyen et al., 2020). Reproduced under the terms of the CC BY license. Note: For Figure A, the scalebars in the HR images correspond to 1 nm. For the EDX colour map, the scale bar corresponds to 60 nm and the colours correspond to: purple-Co, yellow-Cu, red-Ni, orange-Mg, blue-Zn.

capacity of 920 mAh/g after 300 cycles. The HEO was shown to have a Li diffusion coefficient 1-2 orders of magnitude higher than Co_3O_4. The authors attribute the stability of the HEO to the homogeneously distributed inactive MgO. MgO is formed after the initial discharge and is believed to prevent transition metal oxide nanograins from agglomerating during cycling. In addition, sluggish diffusion in the structure reduces agglomeration of secondary particles. They also showed the dependence of electrochemical performance on elemental composition. Other element combinations (such as MgFeTiCuZn-HEO and GaFeCrMnNi-HEO) were shown to have a lower capacity or a more rapid capacity fade.

Lökçü et al. studied the variation of Li content in rock-salt $(MgCoNiZn)_{1-x}Li_xO$ (x = 0.05, 0.15, 0.25, and 0.35) (Lökçü et al., 2020). XPS revealed that an increase in Li content was associated with the oxidation of Co^{2+} to Co^{3+}, and an increase in the concentration of oxygen vacancies to preserve charge neutrality. This had the effect of increasing the discharge capacity, with the best material being $(MgCoNiZn)_{0.65}Li_{0.35}O$ with an initial capacity of 1930 mAh/g. Similar materials have been used as solid electrolytes and are discussed later.

Spinel HEOs have also been shown to provide high capacities when used as anodes. Chen et al. studied spinel $(Mg_{0.2}Ti_{0.2}Zn_{0.2}Cu_{0.2}Fe_{0.2})_3O_4$ as an anode and reported a reversible capacity of 504 mAh/g at a current density of 100 mA/g after 300 cycles (Chen et al., 2020). In addition, the material was able to maintain a capacity around 280 mAh/g for 800 cycles at a high current of 2 A/g. With CV, a large pseudocapacitive contribution of 93% was found at a high scan rate of 1 mV/s. This surface redox process enables a high rate capability. They also observed a reduction in resistance after cycling as evidenced by EIS. Wang et al. studied spinel $(FeCoNiCrMn)_3O_4$ as an anode and optimized the synthesis temperature (D. Wang et al., 2020a). They attribute the

electrochemical performance to mixed valence state metals that induce lattice distortion. The large lattice parameters afforded the material fast diffusion kinetics. Similar to rock-salts, diffraction peaks associated with the spinel structure disappeared during the first lithiation down to 0.01 V, indicating amorphization. Spinel peaks did not reappear after being charged to 3 V. Zhao et al. prepared the $(Co_{0.2}Cr_{0.2}Fe_{0.2}Mn_{0.2}Ni_{0.2})_3O_4$ spinel with a capacity of 428 mAh/g at a high current of 10 A/g (Zhao et al., 2021). The material had a greater discharge capacity and initial CE relative to low and medium entropy derivatives Co_3O_4 and $(Co_{0.25}Cr_{0.25}Fe_{0.25}Mn_{0.25})_3O_4$, respectively. The high-entropy material had the greatest number of oxygen vacancies (as shown by XPS and Electron Paramagnetic Resonance). They attributed the superior performance to these oxygen vacancies, which are believed to accommodate a greater number of Li ions and affect ion migration and electrical conductivity. In addition, thermal stability of the material showed good capacity retention between 0 and 50°C.

Xiang et al. studied spinel $(Al_{0.2}CoCrFeMnNi)_{0.58}O_{4-\delta}$ nanocrystalline powder with a high concentration of oxygen vacancies (Xiang H.-Z. et al., 2021). The material had a porous structure from gas liberation during the combustion synthesis. The inclusion of aluminum in the structure doubled the capacity compared to a $(CoCrFeMnNi)_{0.6}O_4$-δ baseline. This use of inactive Al was inspired by Qiu et al., who showed how the addition of inactive MgO can improve structural stabilization. The authors suggest that small ionic radii Al enhances lattice distortion and allows for the accommodation of more Li. Nanoparticle spinel HEOs have also been prepared with the hydrothermal method (see **Figure 2C**). Nguyen et al. reported a high capacity of 1235 mAh/g and a high number of oxygen vacancies by removing the inactive MgO from the spinel (see **Figure 2D**) (Nguyen et al., 2020). Recently, the same group was able to synthesize the Co-free $(CrMnFeNiCu)_3O_4$ spinel anode (Nguyen et al., 2022). The crystallinity and particle size were varied with post-annealing temperature, and the reported capacities ranged from 600 to 900 mAh/g. Operando XRD also revealed a gradual reduction in peak intensity during the first lithiation, indicative of a collapse in the long-range lattice ordering.

Duan et al. optimized the synthesis of different seven-element $(FeCoNiCrMnXLi)_3O_4$ (X = Cu, Mg, Zn) spinels and used them as anodes (Duan et al., 2021). The Zn-containing spinel had the best performance with a capacity of 522 mAh/g after 100 cycles. They also observed the trend in which the capacity increased gradually during cycling. The beneficial contribution of a single constituent element in spinels has also been studied by Xiao et al. They compared the electrochemical performance of Mg and Zn containing HEOs $(FeNiCrMnZn)_3O_4$ and $(FeNiCrMnMg)_3O_4$ (Xiao et al., 2021). Zn was shown to increase the lithium storage capability, provide a higher amount of trivalent Mn, and improve the crystallinity of the material. In addition, it had a relatively stable capacity of 386 mAh/g at 0.5 A/g after 185 cycles. The same group later prepared the $(FeCoNiCrMn)_3O_4$ spinel anode with a capacity of 596 mAh/g at 2 A/g and 967 mAh/g at 100 mA/g (Xiao et al., 2022). A ball-mill prepared sample of the material had a lower capacity than one prepared via the oxidation of commercial 50 μm HEA powder.

More recent publications on spinels include Tian et al., who prepared the $(CoNiZnXMnLi)_3O_4$ (X = Fe, Cr) anode. The material was tested in full cells and had a specific capacity of 260 mAh/g after 100 cycles at 500 mA/g (Tian et al., 2022). Sun et al. studied the $(Cr_{0.2}Mn_{0.2}Fe_{0.2}Co_{0.2}Ni_{0.2})_3O_4$ spinel, which had a capacity of 560 mAh/g at 100 mA/g (Sun et al., 2022). The pseudocapacitive contribution increased at higher scan rates, as has been reported in other studies (Chen et al., 2019; Wang D. et al., 2020; Zhang et al., 2021; Xiao et al., 2022).

Metallic Alloys

High-entropy alloys are a relatively unexplored research area for the Li-ion battery anode, yet they may mitigate unresolved problems with conventional silicon-based (Si) electrodes. The problem with silicon (and most alloy anodes) is its poor cycle stability. The alloying of lithium and silicon is accompanied with a 300% volume expansion. On a microscopic scale, this causes material swelling, pulverization, and loss of electrical contact with the current collector (Obrovac and Chevrier, 2014). In addition, the continuous formation of solid-electrolyte-interface (SEI) consumes the electrolyte. These problems are responsible for the rapid capacity decay of silicon and alloying materials in batteries.

There has been considerable research on two or three multicomponent alloys with Li for the negative electrode (Obrovac and Chevrier, 2014; Wang X. et al., 2021). Other than Si, common elements that alloy with lithium include Al, Zn, Ga, Ge, Ag, Sn, Sb, and Bi (Obrovac and Chevrier, 2014; Wang X. et al., 2021). For certain systems, varying the compositional ratio can create morphological changes that improve volumetric capacity, as seen with the eutectic Zn-Sn alloy (Heligman et al., 2019). It is known that a multicomponent alloy can improve battery performance relative to a simple binary alloy. For instance, binary alloys with the addition of inactive copper have been shown to improve rate capability and capacity retention (Xin et al., 2017). Ternary alloys with silicon are known to reduce volume expansion and improve performance (Cao et al., 2018). Obrovac et al. reported the preparation and electrochemical performance of 4-component alloys (Obrovac, 2006). They prepared several alloys with silicon, including $Si_{49}Cu_{42}Ag_7Sn_2$, which showed a stable capacity around 1000 mA h/g (Obrovac, 2006). Although not a high-entropy alloy, the material provides insight into the feasibility of multicomponent alloy electrodes. Recently, Ehrenberg's group prepared several high-entropy alloys of the $Gd_{1-x}La_xSn_{2-y}Sb_yM_z$ (M = Li, Na, Mg) system (Pavlyuk et al., 2020). The large atomic size of Gd and La are believed to form voids that may accommodate Li atoms. Their work was mostly fundamental; however, preliminary electrochemical data showed stable cycling. High-entropy alloys have also been used as anode materials in nickel-metal hydride batteries. Edalati et al. studied the $Ti_xZr_{2-x}CrMnFeNi$ alloy with various Ti/Zr ratios (Edalati et al., 2022). The discharge capacity was observed to be dependent on the Ti/Zr ratio, suggesting a wide range of possible electrochemical performances by tuning

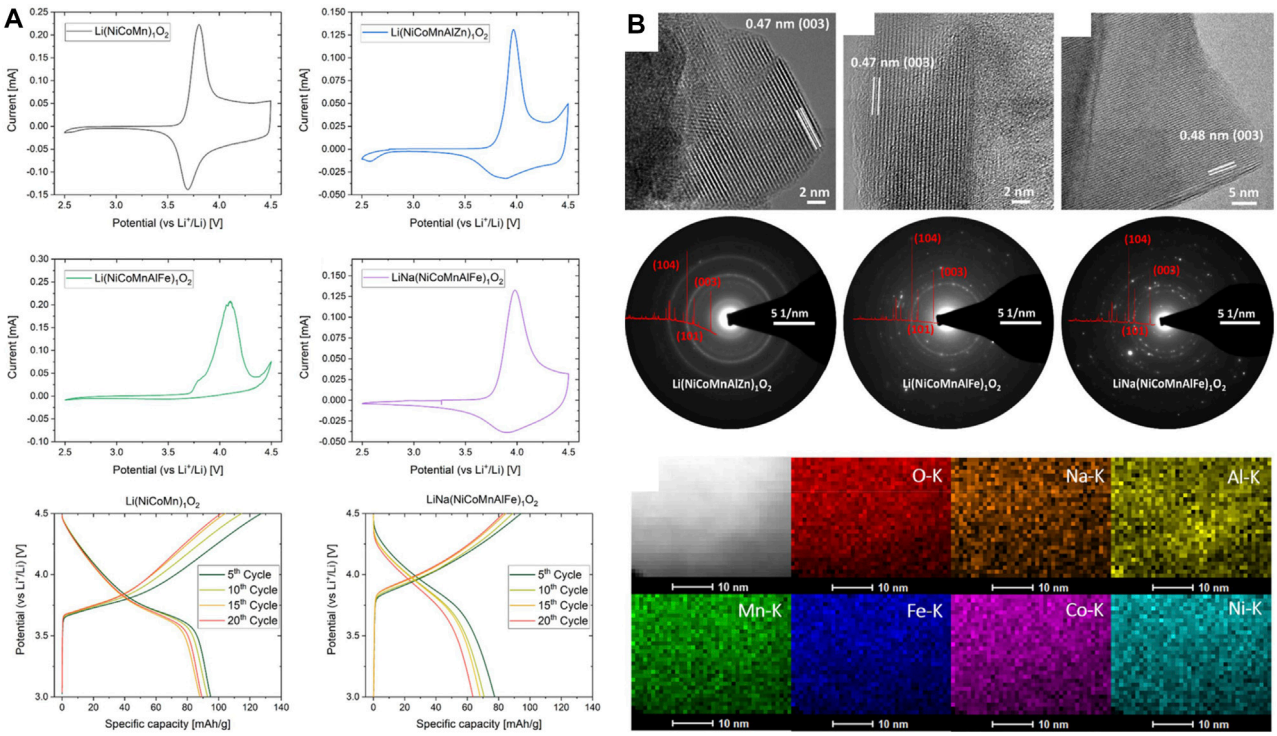

FIGURE 3 | (A) CV and voltage profiles and **(B)** HR-TEM, SAED, and EDX mapping characterization of layered HEO cathode (J. Wang, et al., 2020b). Reproduced under the terms of the CC BY license.

composition. Moreover, the material displayed a low-capacity fade. High-entropy alloys have also been used to accelerate kinetics and increase cycle stability in Li-Sulfur batteries (Xu et al., 2021; Wang Z. et al., 2022). It should be noted that Breitung's group recently prepared and characterized high-entropy sulfides for Li-ion batteries, but the materials had redox activity predominantly around 2 V (Lin et al., 2022).

HIGH-ENTROPY CATHODES

The inclusion of fluorine into high-entropy rock-salts has been shown to increase their working potential to 3.4 V (Wang, et al., 2019b). This should be contrasted with a HEO baseline without fluorine, which has a working potential around 1.0 V. In addition, their preparation is simple and can be done by ball-milling a HEO precursor with LiF. XRD and Nuclear Magnetic Resonance (NMR) confirmed the successful incorporation of Li and F into the structure. These high-entropy rock-salt oxyfluorides have been used as cathode materials for lithium-ion batteries. Wang et al. reported an initial charge capacity of 161 mAh/g at C/10 for $(Li_x(Co_{0.2}Cu_{0.2}Mg_{0.2}Ni_{0.2}Zn_{0.2})OF_x$ (Wang, et al., 2019b). This capacity was higher than a non-entropy stabilized $LiNiOF_x$ baseline, despite containing a greater fraction of redox active nickel. However, the material suffered from a large first cycle irreversible capacity and an overall low CE (Wang, et al., 2019b). The authors attribute this capacity loss to electrolyte degradation, SEI formation, and side reactions. The oxyfluoride had an insertion-type lithiation mechanism, in contrast to the conversion-type mechanism seen in simple HEOs. Mg and Zn were redox inactive and remain divalent as shown with XPS. This cathode also exhibited a capacity increase during cycling.

The same group later studied various layered HEOs including $LiNa(NiCoMnAlFe)_1O_2$ (J. Wang, et al., 2020b). **Figure 3A** shows the material had an oxidation peak at 4.0 V, which is higher than the 3.8 V typically seen for standard $Li(NiCoMn)_1O_2$. However, the electrodes were reported to have a low capacity and a rapid capacity fade (<70 mAh/g after 20 cycles). The incorporation of a small amount of Na ions (**Figure 3B**) was done to improve the battery cycling by widening the diffusion channels. Inclusion of as little as 1 mol% Na (but not K or Rb) has also been reported to marginally improve capacity retention in conventional layered cathodes (He et al., 2019). Recently, Sturman et al. reported similar electrochemical performance for the $Li(NiCoMnTiFe)_1O_2$ layered HEO and observed overlithiation properties that were shown to reduce capacity decay (Sturman et al., 2021). Interestingly, a cathode with the same stoichiometry has also been reported for Na-ion batteries. The cathode was investigated both computationally and experimentally, where it was reported to have a stable capacity of 180 mA h/g (Walczak et al., 2022). Another recent HE layered cathode is described in the work of Wang et al. They used pulsed laser deposition to prepare epitaxial thin films of the layered $LiCr_{1/6}Mn_{1/6}Fe_{1/6}Co_{1/6}Ni_{1/6}Cu_{1/6}O_2$ (K. Wang et al., 2022a). The material was used as a cathode but had low capacity (<60 mAh/g) and high interfacial resistance. Zhen-

Yi Gu et al. made a high-entropy derivative of the NASICON-type fluorophosphate cathode that was shown to increase operating voltage and electrochemical capacity in Na-ion batteries (Gu et al., 2022).

Ceder's group used density functional theory (DFT) to estimate the mixing temperature of different transition metal combinations in cation-disordered rock-salts (DRX) (Lun et al., 2021). As a design strategy, they suggest the incorporation of 30% excess Li and the inclusion of fluorine to increase the redox reservoir. In addition, short-range order (SRO) was suppressed as the number of cations in the DRX increased. SRO was also reported to decrease with increasing synthesis temperature. Their TM6 cathode (i.e. $Li_{1.3}Mn^{2+}_{0.1}Co^{2+}_{0.1}Mn^{3+}_{0.1}Cr^{3+}_{0.1}Ti_{0.1}Nb_{0.2}O_{1.7}F_{0.3}$) had a high initial capacity of 307 mAh/g; however, capacity data was only reported for 20 cycles.

SOLID-STATE ELECTROLYTES

Lithium containing HEO rock-salts have displayed properties that are promising for solid electrolyte applications. Some have been reported to have a Li-ion conductivity several orders of magnitude greater than LiPON (Bérardan et al., 2016). Bérardan et al. studied the room-temperature ionic conductivity of rock-salt $(MgCoNiCuZn)_{1-x-y}Ga_yA_xO$ (with A = Li, Na, K) and reported a value exceeding 10^{-3} S cm^{-1} (Bérardan et al., 2016). Later, the team studied $(MgCoNiCuZn)_{1-x}Li_xO$ with varying concentrations of Li. They identified a charge compensation mechanism that begins with the oxidation of Co^{2+} to Co^{3+}, followed by the formation of oxygen vacancies when the Li fraction exceeds x = 0.21 (Osenciat et al., 2019). High-entropy electrolytes have also been applied to Na-ion batteries, such as HE NASICON phosphate electrolytes (Wu et al., 2022).

Recent work on solid electrolytes includes HE garnets, argyrodites, and perovskites. Stockham et al. reported the successful synthesis of Ga-containing lithium garnet electrolytes composed of 9 and 11 elements (e.g., $Ga_{0.2}Li_{5.75}La_{2.5}Nd_{0.5}Nb_{0.65}Ce_{0.1}Zr_1Ti_{0.25}O_{12}$) (Stockham, Dong and Slater, 2022). The electrolytes were simple to prepare and had both good room temperature conductivity (0.2 mS cm^{-1}) and stability. As we have seen, most current research targets a high configurational entropy for the cations. However, recent work by Strauss et al. reports HE-polyanionic argyrodite-type solid electrolytes (Strauss et al., 2022). Unlike most publications, the authors reported a nonuniform distribution of elements. The high entropy was reported to lower activation energy for conduction but did not significantly affect ionic conductivity. Equimolar high-entropy perovskite electrolytes with varying Al content were reported but had a conductivity on the order of 10^{-7} S cm^{-1} (Yazhou and Zhiren, 2022). The authors also investigated the material as an anode, however the use of heavy elements (i.e. La and Ba) resulted in a low capacity of 58 mAh/g. Other studies have also used perovskites as electrode materials. Yan et al. reported results for the less-studied high-entropy perovskite titanate (Yan et al., 2020). It had an initial capacity of 125 mAh/g followed by a large irreversible capacity, but a stable capacity of 80 mA h/g. The perovskite also had a gradual increase in capacity over 300 cycles, which the authors attribute to the gradual penetration of the electrolyte into the electrode and the formation of a gel-like film.

ADVANCED CHARACTERIZATION AND STORAGE MECHANISM

Confirmation of the homogeneous elemental distribution in HEOs has been an important part of their characterization since Rost et al. It has traditionally been supported with EDX or XRD analysis on the bulk powder. However, this may not be sufficient to detect traces of secondary phases or localized heterogeneities, which can affect the material's property and electrochemical performance. Chellali et al. used Atomic Probe Tomography (APT) to study the atomic scale homogeneity of various transition metal, rare-earth metal, and perovskite-based HEOs prepared by a high-pressure compact method (Chellali et al., 2019). Their results confirm the random and homogeneous distribution of cations at the atomic level.

Moździerz et al. studied lattice distortion effects in $(CoCuMgNiZn)_{1-x}Li_xO$ by increasing lithium levels during synthesis (x = 0–0.3) (Moździerz et al., 2021). The internal strain increased up to a Li composition of 0.2, after which the introduction of more Li released the internal strain through the formation of oxygen vacancies. The compound displayed mixed ionic-electronic conductivity upon the insertion of Li. Different mechanisms were proposed: intercalation-based insertion at high voltage and conversion or alloying at low voltage. Cheng et al. studied the effects of pressure on lattice distortion in $(Ce_{0.2}La_{0.2}Pr_{0.2}Sm_{0.2}Y_{0.2})O_{2-\delta}$ HEO (Cheng et al., 2019). They observed pressure-induced transformations from the crystal state to the amorphous state below the melting point or glass-transition temperature. This property may allow for the development of ceramic-glass composites with applications in solid-state electrolytes.

Since 2018, authors have reported details regarding the partial conversion reaction in rock-salt HEOs. Sarkar suggested that certain cations (Co^{2+} and Cu^{2+}) are involved in the conversion, whereas other cations (Mg^{2+}) stabilize the structure (Sarkar, et al., 2018a). Operando XRD in **Figure 4A** shows the typical behaviour of a HE-rock-salt upon lithiation. Reflections from the rock-salt structure disappeared during the first lithiation due to the "formation of small crystallites" (which is often seen in conversion materials) (Sarkar, et al., 2018a). However, Selected Area Electron Diffraction (SAED) was still able to detect trace reflections from the rock-salt structure, providing evidence of a partially preserved structure that enables reversible lithium storage (Sarkar, et al., 2018a). Similar observations have been made in subsequent studies. Tavani et al. studied the lithiation mechanism of HEO $(Mg_{0.2}Co_{0.2}Ni_{0.2}Cu_{0.2}Zn_{0.2})O$ with operando X-ray Absorption Spectroscopy (XAS) to quantify the reduction of transition metal species (Tavani et al., 2020). For this material, upon lithiation, Cu^{2+} is first reduced to a mixture of 62% metallic Cu and 32% Cu_2O. Then, 75% of the Ni^{2+} is reduced to metallic Ni. Finally, around 62% of the Co^{2+} is reduced to

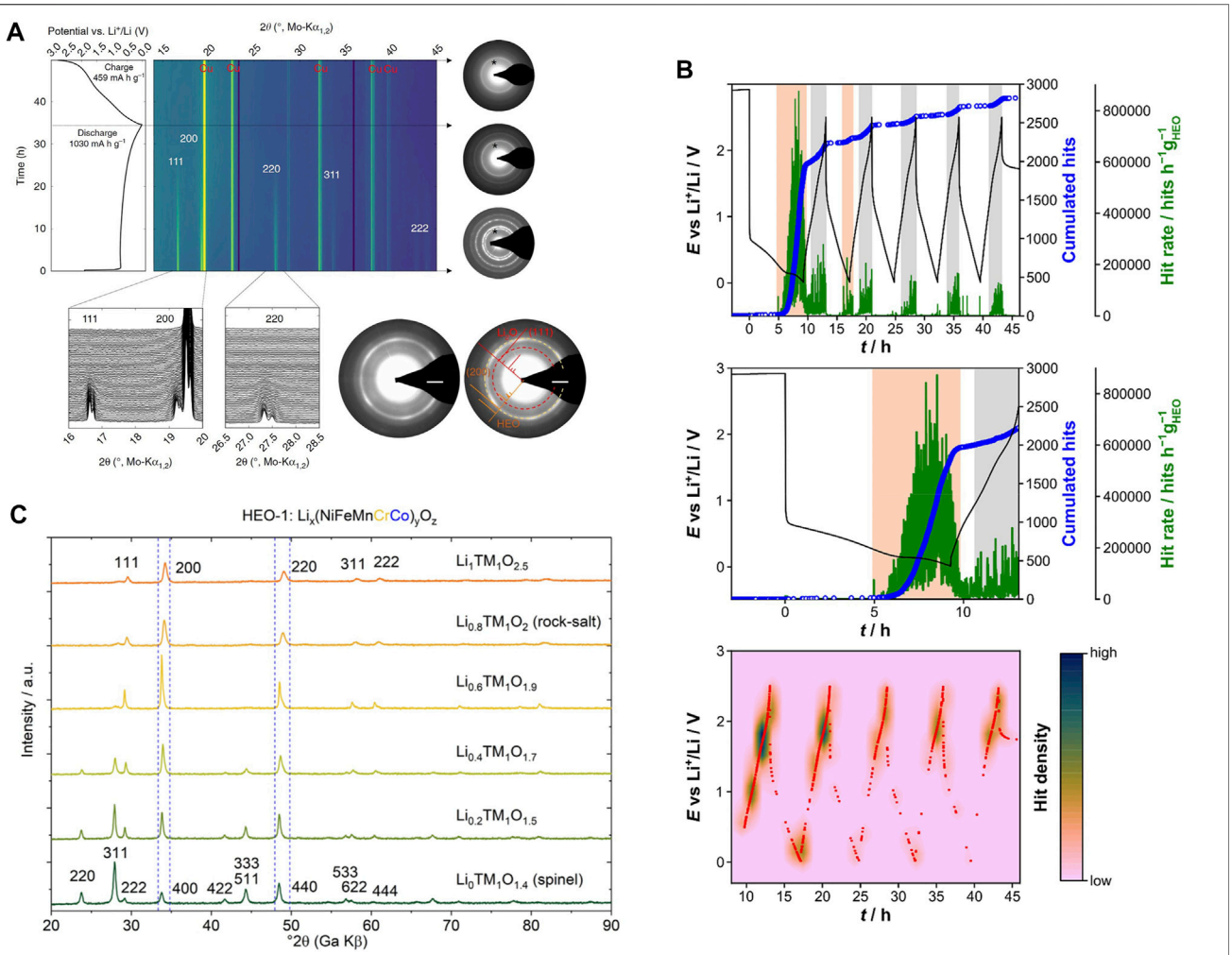

FIGURE 4 | (A) Operando XRD of $(Co_{0.2}Cu_{0.2}Mg_{0.2}Ni_{0.2}Zn_{0.2})O$ anode (Sarkar, et al., 2018a). **(B)** Operando AE investigation of HEO anode (Schweidler et al., 2021). **(C)** XRD of the spinel to rock-salt transformation seen with high lithium concentrations (J. Wang, et al., 2020c). Reproduced under the terms of the CC BY license.

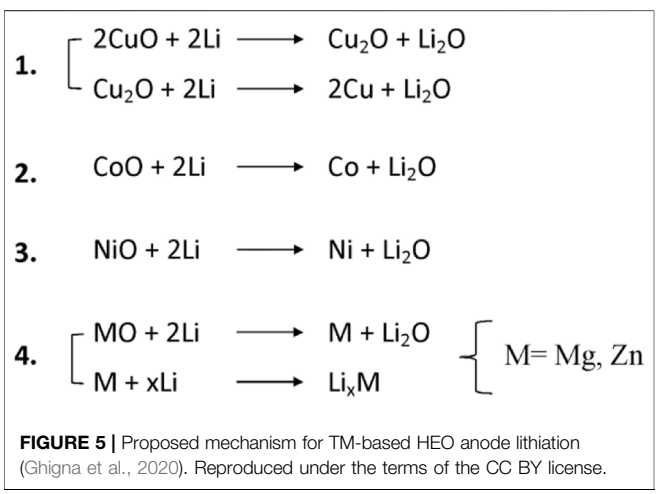

FIGURE 5 | Proposed mechanism for TM-based HEO anode lithiation (Ghigna et al., 2020). Reproduced under the terms of the CC BY license.

metallic Co. The order of this sequence was noted to follow the redox potential of each element. These observations are also consistent with the work of Ghigna et al., where a lithiation/delithiation mechanism for $(Mg_{0.2}Co_{0.2}Ni_{0.2}Cu_{0.2}Zn_{0.2})O$ is proposed (Ghigna et al., 2020). The mechanism is illustrated in **Figure 5**.

They suggest a two-stage process beginning with the conversion of cations (Cu^{2+}, Co^{2+}, Ni^{2+}), followed by the conversion and eventual alloying/de-alloying of Mg^{2+} and Zn^{2+}. Surprisingly, it was found that ZnO is also involved in the conversion mechanism, as shown by the presence of metallic Zn. The reaction is incomplete and irreversible and ultimately leads to a collapse of the rock-salt structure, although 60% of the capacity remains. Wang et al. studied different quantities of Mg in the structure of $(Mg_{0.2}Co_{0.2}Ni_{0.2}Cu_{0.2}Zn_{0.2})O$ and found homogeneous single-phase compounds for only the Mg-containing oxides (Wang S.-Y. et al., 2021). However, the Mg-free sample still had good electrochemical performance. Operando X-Ray Microscope Spectroscopy revealed greater amounts of Mg were associated with a reduced pulverization.

More detailed characterization regarding HEO degradation is found in the work of Schweidler and Breitung. Schweidler et al.

studied the lithiation of the $(Co_{0.2}Cu_{0.2}Mg_{0.2}Ni_{0.2}Zn_{0.2})O$ anode with Acoustic Emission (AE) monitoring (**Figure 4B**) (Schweidler et al., 2021). The first cycle showed strong AE activity at low voltage, which was attributed to SEI formation. Later, they observed AEs mostly during the delithiation cycles, which is often where there are mechanical stresses associated with alloying/dealloying. Schweidler et al. also studied high-entropy oxyfluorides with AE (Schweidler et al., 2022). Acoustic activity was most prominent during the first cycle above 4.6 V and was attributed to mechanical degradation (crack propagation) and gas evolution. Further insight into the lithiation behaviour and side reactions that occur during the first cycle can be revealed by the gases released during cycling. For instance, oxygen release during cycling can be due to a phase transition in cathode materials. Breitung et al. investigated the gassing behaviour of the $Li(Co_{0.2}Cu_{0.2}Mg_{0.2}Ni_{0.2}Zn_{0.2})OF$ cathode and the $(Co_{0.2}Cu_{0.2}Mg_{0.2}Ni_{0.2}Zn_{0.2})O$ anode with the help of pressure measurements and Differential Electrochemical Mass Spectrometry (DEMS) (Breitung et al., 2020). The anode evolved C_2H_4 gas mostly during the first cycle, which was attributed to the formation of a stable SEI. This was observed without the need for additives in the electrolyte, which are typically used in other high-capacity anodes like silicon. For the cathode, gassing behaviour was dependent on cut-off voltage. Onset of gas evolution was seen as early as 4.55 V for CO_2, however the 5 V cutoff was associated with the greatest gas evolution involving CO_2, CO, H_2, O_2, and POF_3. CO_2 and CO were attributed to oxidation of the electrolyte, which yields decomposition products that later form H_2. The $LiPF_6$ salt decomposition produced POF_3, and O_2 evolution was associated with surface lattice oxygen release. These observations are consistent with a mechanism similar to Li-rich disordered rock-salts. (Breitung et al., 2020).

Spinels are known to convert to rock-salt during synthesis upon the addition of lithium, as seen in **Figure 4C**. Wang et al. investigated the spinel to rock-salt transformation that occurs upon the incorporation of Li into HEOs during synthesis (J. Wang, et al., 2020c). The addition of lithium was accompanied with the oxidation of transition metals until oxidation was no longer possible, resulting in the transformation to rock-salt. The phase conversion in spinel $(CrMnFeCoNi)_3O_4$ during electrochemical cycling has also been studied at the atomic scale (Huang et al., 2021). During lithiation, the authors observed the formation of $Cr_xFe_{3-x}O_4$ and $LiNi_xCo_{1-x}O_2$ phases along with metallic Mn nanocrystals at 0.5 V. Further lithiation to 0.01 V led to the emergence of metallic Fe, Cr, Co., and Ni. Upon delithiation, the remaining spinel grains grew by incorporating nearby metal nanoparticles.

Several publications have studied the magnetic properties of HEOs. Witte et al. studied the magnetic properties of perovskite-type HEOs with rare-earth metals and observed mostly antiferromagnetic behaviour (Witte et al., 2019, 2020). More recently, Sarkar et al. reviewed the magnetic properties of HEOs (Sarkar, Kruk and Hahn, 2021). Sarkar also studied the electronic band structure of rare-earth metal based fluorite HEOs (Sarkar et al., 2020a). They highlighted the importance of synthesis temperature and atmosphere (reducing/oxidizing gas) on the band structure and number of oxygen vacancies.

SUMMARY AND OUTLOOK

The field of electrochemical energy storage has seen a recent growth in high-entropy materials. HEOs have the potential to be used as anode materials in Li-ion batteries as they offer very high capacity compared to the conventional graphite anode limited to 372 mAh/g. However, it must be stressed that these oxides typically have a large first cycle irreversible capacity and an electrochemical stability that is inferior to traditional anodes. In addition, they tend to operate at a higher potential (1 V—2 V) than graphite (0.2 V—0.3 V). For most applications, this is too high as it significantly drops the output voltage of the battery when coupled with conventional NMC layered cathodes (at around 4 V). Also, non-faradaic and surface pseudocapacitive contributions to the total capacity are still not fully understood. The presence of multiple cations, many of which have good catalytic activity, may react with the organic solvents and salts of the electrolytes. Alternatively, these novel electrode-electrolyte interactions may prove beneficial, as they may enable the formation of a highly stable SEI.

Disorder in cathode materials is known in the battery field to be a largely detrimental property. A classic example is $LiNiO_2$, where significant Li-Ni cation mixing causes degradation and eventual phase transition. The addition of other metal cations (i.e., Mn and Co.) has proven successful, as in the case of commercial NMC111. Here, stability was improved by these metal cations, and more careful cation selection may improve structural stability even further. However, it is not yet clear whether entropy stabilized cathodes are any less susceptible to degradation. In addition, certain promising high-capacity cathodes like DRXs require processing under argon which may limit their commercial viability. Nevertheless, HEO cathodes have the potential to stabilize the structure and allow metal cations to have greater stability and site energies that accommodate lithium. The use of five metal cations, without or with fluorination (such as in the case of DRX), or layered structures along with vacancies could lead to stable fully de-lithiated cathodes and hence higher capacities. Compared to HE-anodes, there is little work on HE-cathodes. Further work is needed to explore the full potential of these novel electrodes.

Finally, HEAs offer new opportunities to solve the challenges associated with conventional high-capacity anodes like silicon or lithium metal. Compared to HE-oxides, there is little research regarding HE-alloys for anode materials. Although it is unlikely that entropy stabilization would eliminate the swelling associated with Li alloying, HEAs may reduce capacity fade in otherwise high-capacity anodes. Researchers should consider strategies such as the combination of alloying (e.g., Sn, Al) and inert/non-alloying elements (e.g., Cu), and the use of elements with a large atomic radius (e.g., La). The practical and economic

feasibility of the latter option is increased if the composition is not limited to strict equiatomic proportions.

In recent years, high-entropy materials have been employed in numerous fields of energy research, but more work needs to be done. Given the complexity of these materials, it is expected that computational techniques and high-throughput experimentation will play a key role in the future of the material design cycle. However, this outlook should be approached critically. Computational design strategies arise out of pre-existing paradigms and may overlook truly novel materials. For instance, high-throughput studies on HE-*rock-salts* may direct resources away from the discovery of entirely new families of HE structures. Additional challenges are related to the collection of high-quality data (a prerequisite for the successful implementation of machine learning). Ideally, high-throughput experimentation will be used in conjunction with computational designs and the more *traditional* experimental exploration.

AUTHOR CONTRIBUTIONS

JS: research and writing. YA-L and EB: editing and revisions.

ACKNOWLEDGMENTS

We would like to thank the Office of Energy Research and Development (OERD) at Natural Resources Canada for financial support.

REFERENCES

Akrami, S., Edalati, P., Fuji, M., and Edalati, K. (2021). High-Entropy Ceramics: Review of Principles, Production and Applications. *Mater. Sci. Eng. R Rep.* 146 (August), 100644. doi:10.1016/j.mser.2021.100644

Amiri, A., and Shahbazian-Yassar, R. (2021). Recent Progress of High-Entropy Materials for Energy Storage and Conversion. *J. Mat. Chem. A* 9, 782–823. doi:10.1039/d0ta09578h

Anik, M., and Lokcu, E. (2019). Synthesis and Electrochemical Performance of the $(Mg_{0.2}Co_{0.2}Ni_{0.2}Zn_{0.2}Li_{0.2})$ O High Entropy Oxide as Anode Material for Li-Ion Batteries. *Eurasia Proc. Sci. Technol. Eng. Math.* 7, 329–332. Available at: https://dergipark.org.tr/tr/pub/epstem/issue/50288/656424.

Bérardan, D., Franger, S., Meena, A. K., and Dragoe, N. (2016). Room Temperature Lithium Superionic Conductivity in High Entropy Oxides. *J. Mat. Chem. A* 4 (24), 9536–9541. doi:10.1039/c6ta03249d

Breitung, B., Wang, Q., Schiele, A., Tripković, Đ., Sarkar, A., Velasco, L., et al. (2020). Gassing Behavior of High-Entropy Oxide Anode and Oxyfluoride Cathode Probed Using Differential Electrochemical Mass Spectrometry. *Batter. Supercaps* 3 (4), 361–369. doi:10.1002/batt.202000010

Cantor, B., Chang, I. T. H., Knight, P., and Vincent, A. J. B. (2004). Microstructural Development in Equiatomic Multicomponent Alloys. *Mater. Sci. Eng. A* 375-377 (1-2), 213–218. doi:10.1016/j.msea.2003.10.257

Cao, Y., Scott, B., Dunlap, R. A., and Obrovac, M. N. (2018). Mechanically Milled Si-Mn-Fe Alloys as Negative Electrodes for Li-Ion Batteries. *Meet. Abstr.* MA2018-01, 393. doi:10.1149/MA2018-01/3/393

Chellali, M. R., Sarkar, A., Nandam, S. H., Bhattacharya, S. S., Breitung, B., Hahn, H., et al. (2019). On the Homogeneity of High Entropy Oxides: An Investigation at the Atomic Scale. *Scr. Mater.* 166, 58–63. doi:10.1016/j.scriptamat.2019.02.039

Chen, H., Qiu, N., Wu, B., Yang, Z., Sun, S., and Wang, Y. (2020). A New Spinel High-Entropy Oxide $(Mg_{0.2}Ti_{0.2}Zn_{0.2}Cu_{0.2}Fe_{0.2})_3O_4$ with Fast Reaction Kinetics and Excellent Stability as an Anode Material for Lithium Ion Batteries. *RSC Adv.* 10 (16), 9736–9744. doi:10.1039/d0ra00255k

Chen, H., Qiu, N., Wu, B., Yang, Z., Sun, S., and Wang, Y. (2019). Tunable Pseudocapacitive Contribution by Dimension Control in Nanocrystalline-Constructed $(Mg_{0.2}Co_{0.2}Ni_{0.2}Cu_{0.2}Zn_{0.2})$O Solid Solutions to Achieve Superior Lithium-Storage Properties. *RSC Adv.* 9 (50), 28908–28915. doi:10.1039/c9ra05508h

Chen, Y., Fu, H., Huang, Y., Huang, L., Zheng, X., Dai, Y., et al. (2021). Opportunities for High-Entropy Materials in Rechargeable Batteries. *ACS Mater. Lett.* 3 (2), 160–170. doi:10.1021/acsmaterialslett.0c00484

Cheng, B., Lou, H., Sarkar, A., Zeng, Z., Zhang, F., Chen, X., et al. (2019). Pressure-Induced Tuning of Lattice Distortion in a High-Entropy Oxide. *Commun. Chem.* 2 (1), 1–9. doi:10.1038/s42004-019-0216-2

Djenadic, R., Sarkar, A., Clemens, O., Loho, C., Botros, M., Chakravadhanula, V. S. K., et al. (2017). Multicomponent Equiatomic Rare Earth Oxides. *Mater. Res. Lett.* 5 (2), 102–109. doi:10.1080/21663831.2016.1220433

Dong, Q., Hong, M., Gao, J., Li, T., Cui, M., Li, S., et al. (2022). Rapid Synthesis of High-Entropy Oxide Microparticles. *Small* 18 (11), 2104761. doi:10.1002/smll.202104761

Duan, C., Tian, K., Li, X., Wang, D., Sun, H., Zheng, R., et al. (2021). New Spinel High-Entropy Oxides $(FeCoNiCrMnXLi)_3O_4$ (X = Cu, Mg, Zn) as the Anode Material for Lithium-Ion Batteries. *Ceram. Int.* 47 (22), 32025–32032. doi:10.1016/j.ceramint.2021.08.091

Duncan, H., Courtel, F. M., and Abu-Lebdeh, Y. (2015). A Study of the Solid-Electrolyte-Interface (SEI) of $ZnMn_2O_4$: A Conversion-Type Anode Material for Li-Ion Batteries. *J. Electrochem. Soc.* 162 (13), A7110–A7117. doi:10.1149/2.0141513jes

Edalati, P., Mohammadi, A., Li, Y., Li, H.-W., Floriano, R., Fuji, M., et al. (2022). High-Entropy Alloys as Anode Materials of Nickel - Metal Hydride Batteries. *Scr. Mater.* 209, 114387. doi:10.1016/j.scriptamat.2021.114387

Etman, A. S., Zhou, J., and Rosen, J. (2022). Ti1.1V0.7Cr $Nb_{1.0}Ta_{0.6}C_3T$ High-Entropy MXene Freestanding Films for Charge Storage Applications. *Electrochem. Commun.* 137 (February), 107264. doi:10.1016/j.elecom.2022.107264

Fu, M., Ma, X., Zhao, K., Li, X., and Su, D. (2021). High-Entropy Materials for Energy-Related Applications. *iScience* 24 (3), 102177. doi:10.1016/j.isci.2021.102177

Ghigna, P., Airoldi, L., Fracchia, M., Callegari, D., Anselmi-Tamburini, U., D'Angelo, P., et al. (2020). Lithiation Mechanism in High-Entropy Oxides as Anode Materials for Li-Ion Batteries: An Operando XAS Study. *ACS Appl. Mat. Interfaces* 12 (45), 50344–50354. doi:10.1021/acsami.0c13161

Gu, Z. Y., Guo, J. Z., Cao, J. M., Wang, X. T., Zhao, X. X., Zheng, X. Y., et al. (2022). An Advanced High-Entropy Fluorophosphate Cathode for Sodium-Ion Batteries with Increased Working Voltage and Energy Density. *Adv. Mater.* 34 (14), 2110108. doi:10.1002/adma.202110108

Guo, H., Shen, J., Wang, T., Cheng, C., Yao, H., Han, X., et al. (2022). Design and Fabrication of High-Entropy Oxide Anchored on Graphene for Boosting Kinetic Performance and Energy Storage. *Ceram. Int.* 48 (3), 3344–3350. doi:10.1016/j.ceramint.2021.10.109

He, T., Chen, L., Su, Y., Lu, Y., Bao, L., Chen, G., et al. (2019). The Effects of Alkali Metal Ions with Different Ionic Radii Substituting in Li Sites on the Electrochemical Properties of Ni-Rich Cathode Materials. *J. Power Sources* 441 (October), 227195. doi:10.1016/j.jpowsour.2019.227195

Heligman, B. T., Kreder, K. J., Scanlan, K. P., Sun, R., and Manthiram, A. (2019). Interdigitated Eutectic Alloy Anodes with High-Volumetric Capacity for Lithium-Ion Batteries. *Meet. Abstr.* MA2019-01, 249. doi:10.1149/MA2019-01/2/249

Huang, C.-Y., Huang, C.-W., Wu, M.-C., Patra, J., Xuyen Nguyen, T., Chang, M.-T., et al. (2021). Atomic-Scale Investigation of Lithiation/Delithiation Mechanism in High-Entropy Spinel Oxide with Superior Electrochemical Performance. *Chem. Eng. J.* 420 (April), 129838. doi:10.1016/j.cej.2021.129838

Kheradmandfard, M., Minouei, H., Tsvetkov, N., Vayghan, A. K., Kashani-Bozorg, S. F., Kim, G., et al. (2021). Ultrafast Green Microwave-Assisted Synthesis of High-Entropy Oxide Nanoparticles for Li-Ion Battery Applications. *Mater. Chem. Phys.* 262 (January), 124265. doi:10.1016/j.matchemphys.2021.124265

Lin, L., Wang, K., Sarkar, A., Njel, C., Karkera, G., Wang, Q., et al. (2022). High-Entropy Sulfides as Electrode Materials for Li-Ion Batteries. *Adv. Energy Mater.* 12 (8), 2103090. doi:10.1002/aenm.202103090

Lin, Y., Luo, N., Chamas, M., Hu, C., and Grasso, S. (2021). Sustainable High-Entropy Ceramics for Reversible Energy Storage: A Short Review. *Int. J. Appl. Ceram. Technol.* 18 (5), 1560–1569. doi:10.1111/ijac.13762

Lökçü, E., Toparli, Ç., and Anik, M. (2020). Electrochemical Performance of $(MgCoNiZn)_{1-x}Li_xO$ High-Entropy Oxides in Lithium-Ion Batteries. *ACS Appl. Mat. Interfaces* 12 (21), 23860–23866. doi:10.1021/acsami.0c03562

Lun, Z., Ouyang, B., Kwon, D.-H., Ha, Y., Foley, E. E., Huang, T.-Y., et al. (2021). Cation-Disordered Rocksalt-Type High-Entropy Cathodes for Li-Ion Batteries. *Nat. Mat.* 20 (2), 214–221. doi:10.1038/s41563-020-00816-0

Ma, Y., Ma, Y., Wang, Q., Schweidler, S., Botros, M., Fu, T., et al. (2021). High-Entropy Energy Materials: Challenges and New Opportunities. *Energy Environ. Sci.* 14 (5), 2883–2905. doi:10.1039/d1ee00505g

Możdzierz, M., Dąbrowa, J., Stępień, A., Zajusz, M., Stygar, M., Zając, W., et al. (2021). Mixed Ionic-Electronic Transport in the High-Entropy $(Co,Cu,Mg,Ni,Zn)_1$-Li O Oxides. *Acta Mater.* 208, 116735. doi:10.1016/j.actamat.2021.116735

Nemani, S. K., Zhang, B., Wyatt, B. C., Hood, Z. D., Manna, S., Khaledialidusti, R., et al. (2021). High-Entropy 2D Carbide MXenes: $TiVNbMoC_3$ and $TiVCrMoC_3$. *ACS Nano* 15 (8), 12815–12825. doi:10.1021/acsnano.1c02775

Nguyen, T. X., Patra, J., Chang, J.-K., and Ting, J.-M. (2020). High Entropy Spinel Oxide Nanoparticles for Superior Lithiation-Delithiation Performance. *J. Mat. Chem. A* 8 (36), 18963–18973. doi:10.1039/d0ta04844e

Nguyen, T. X., Tsai, C.-C., Patra, J., Clemens, O., Chang, J.-K., and Ting, J.-M. (2022). Co-Free High Entropy Spinel Oxide Anode with Controlled Morphology and Crystallinity for Outstanding Charge/Discharge Performance in Lithium-Ion Batteries. *Chem. Eng. J.* 430 (P1), 132658. doi:10.1016/j.cej.2021.132658

Nitta, N., Wu, F., Lee, J. T., and Yushin, G. (2015). Li-Ion Battery Materials: Present and Future. *Mater. Today* 18 (5), 252–264. doi:10.1016/j.mattod.2014.10.040

Obrovac, M. N., and Chevrier, V. L. (2014). Alloy Negative Electrodes for Li-Ion Batteries. *Chem. Rev.* 114 (23), 11444–11502. doi:10.1021/cr500207g

Obrovac, M. (2006). WO2006028583A2. USA: World International Property Organization.

Osenciat, N., Bérardan, D., Dragoe, D., Léridon, B., Holé, S., Meena, A. K., et al. (2019). Charge Compensation Mechanisms in Li-Substituted High-Entropy Oxides and Influence on Li Superionic Conductivity. *J. Am. Ceram. Soc.* 102 (10), 6156–6162. doi:10.1111/jace.16511

Pavlyuk, V., Balińska, A., Rożdżyńska-Kiełbik, B., Pavlyuk, N., Dmytriv, G., Stetskiv, A., et al. (2020). New Maximally Disordered - High Entropy Intermetallic Phases (MD-HEIP) of the $Gd_{1-x}La_xSn_{2-y}SbyMz$ (M=Li, Na, Mg): Synthesis, Structure and Some Properties. *J. Alloys Compd.* 838, 155643. doi:10.1016/j.jallcom.2020.155643

Pickering, E. J., and Jones, N. G. (2016). High-Entropy Alloys: A Critical Assessment of Their Founding Principles and Future Prospects. *Int. Mater. Rev.* 61 (3), 183–202. doi:10.1080/09506608.2016.1180020

Qiu, N., Chen, H., Yang, Z., Sun, S., Wang, Y., and Cui, Y. (2019). A High Entropy Oxide $(Mg_{0.2}Co_{0.2}Ni_{0.2}Cu_{0.2}Zn_{0.2}O)$ with Superior Lithium Storage Performance. *J. Alloys Compd.* 777, 767–774. doi:10.1016/j.jallcom.2018.11.049

Rost, C. M., Sachet, E., Borman, T., Moballegh, A., Dickey, E. C., Hou, D., et al. (2015). Entropy-Stabilized Oxides. *Nat. Commun.* 6 (1), 8485. doi:10.1038/ncomms9485

Sarkar, A., Breitung, B., and Hahn, H. (2020b). High Entropy Oxides: The Role of Entropy, Enthalpy and Synergy. *Scr. Mater.* 187, 43–48. doi:10.1016/j.scriptamat.2020.05.019

Sarkar, A., Djenadic, R., Usharani, N. J., Sanghvi, K. P., Chakravadhanula, V. S. K., Gandhi, A. S., et al. (2017b). Nanocrystalline Multicomponent Entropy Stabilised Transition Metal Oxides. *J. Eur. Ceram. Soc.* 37 (2), 747–754. doi:10.1016/j.jeurceramsoc.2016.09.018

Sarkar, A., Djenadic, R., Wang, D., Hein, C., Kautenburger, R., Clemens, O., et al. (2018b). Rare Earth and Transition Metal Based Entropy Stabilised Perovskite Type Oxides. *J. Eur. Ceram. Soc.* 38 (5), 2318–2327. doi:10.1016/j.jeurceramsoc.2017.12.058

Sarkar, A., Eggert, B., Velasco, L., Mu, X., Lill, J., Ollefs, K., et al. (2020a). Role of Intermediate 4f States in Tuning the Band Structure of High Entropy Oxides. *Apl. Mater.* 8 (5), 051111. doi:10.1063/5.0007944

Sarkar, A., Kruk, R., and Hahn, H. (2021). Magnetic Properties of High Entropy Oxides. *Dalton Trans.* 50 (6), 1973–1982. doi:10.1039/d0dt04154h

Sarkar, A., Loho, C., Velasco, L., Thomas, T., Bhattacharya, S. S., Hahn, H., et al. (2017a). Multicomponent Equiatomic Rare Earth Oxides with a Narrow Band Gap and Associated Praseodymium Multivalency. *Dalton Trans.* 46 (36), 12167–12176. doi:10.1039/C7DT02077E

Sarkar, A., Velasco, L., Wang, D., Wang, Q., Talasila, G., de Biasi, L., et al. (2018a). High Entropy Oxides for Reversible Energy Storage. *Nat. Commun.* 9 (1), 3400. doi:10.1038/s41467-018-05774-5

Sarkar, A., Wang, Q., Schiele, A., Chellali, M. R., Bhattacharya, S. S., Wang, D., et al. (2019). High-Entropy Oxides: Fundamental Aspects and Electrochemical Properties. *Adv. Mat.* 31 (26), 1806236. doi:10.1002/adma.201806236

Schweidler, S., Dreyer, S. L., Breitung, B., and Brezesinski, T. (2022). Acoustic Emission Monitoring of High-Entropy Oxyfluoride Rock-Salt Cathodes During Battery Operation. *Coatings* 12 (3), 402. doi:10.3390/coatings12030402

Schweidler, S., Dreyer, S. L., Breitung, B., and Brezesinski, T. (2021). Operando Acoustic Emission Monitoring of Degradation Processes in Lithium-Ion Batteries with a High-Entropy Oxide Anode. *Sci. Rep.* 11 (1), 1–8. doi:10.1038/s41598-021-02685-2

Stockham, M. P., Dong, B., and Slater, P. R. (2022). High Entropy Lithium Garnets - Testing the Compositional Flexibility of the Lithium Garnet System. *J. Solid State Chem.* 308 (December), 122944. doi:10.1016/j.jssc.2022.122944

Strauss, F., Lin, J., Duffiet, M., Wang, K., Zinkevich, T., Hansen, A.-L., et al. (2022). High-Entropy Polyanionic Lithium Superionic Conductors. *ACS Mater. Lett.* 4 (2), 418–423. doi:10.1021/acsmaterialslett.1c00817

Sturman, J., Yim, C.-H., Baranova, E. A., and Abu-Lebdeh, Y. (2021). Communication-Design of $LiNi_{0.2}Mn_{0.2}Co_{0.2}Fe_{0.2}Ti_{0.2}O_2$ as a High-Entropy Cathode for Lithium-Ion Batteries Guided by Machine Learning. *J. Electrochem. Soc.* 168 (5), 050541. doi:10.1149/1945-7111/ac00f4

Sun, Z., Zhao, Y., Sun, C., Ni, Q., Wang, C., and Jin, H. (2022). High Entropy Spinel-Structure Oxide for Electrochemical Application. *Chem. Eng. J.* 431 (July), 133448. doi:10.1016/j.cej.2021.133448

Tavani, F., Fracchia, M., Pianta, N., Ghigna, P., Quartarone, E., and D'Angelo, P. (2020). Multivariate Curve Resolution Analysis of Operando XAS Data for the Investigation of the Lithiation Mechanisms in High Entropy Oxides. *Chem. Phys. Lett.* 760 (August), 137968. doi:10.1016/j.cplett.2020.137968

Tian, K.-H., Duan, C.-Q., Ma, Q., Li, X.-L., Wang, Z.-Y., Sun, H.-Y., et al. (2022). High-Entropy Chemistry Stabilizing Spinel Oxide $(CoNiZnXMnLi)_3O_4$ (X = Fe, Cr) for High-Performance Anode of Li-Ion Batteries. *Rare Met.* 41 (4), 1265–1275. doi:10.1007/s12598-021-01872-4

Vaidya, M., Muralikrishna, G. M., and Murty, B. S. (2019). High-Entropy Alloys by Mechanical Alloying: A Review. *J. Mat. Res.* 34 (5), 664–686. doi:10.1557/jmr.2019.37

Walczak, K., Plewa, A., Ghica, C., Zając, W., Trenczek-Zając, A., Zając, M., et al. (2022). $NaMn_{0.2}Fe_{0.2}Co_{0.2}Ni_{0.2}Ti_{0.2}O_2$ High-Entropy Layered Oxide - Experimental and Theoretical Evidence of High Electrochemical Performance in Sodium Batteries. *Energy Storage Mater.* 47 (December 2021), 500–514. doi:10.1016/j.ensm.2022.02.038

Wang, D., Jiang, S., Duan, C., Mao, J., Dong, Y., Dong, K., et al. (2020a). Spinel-Structured High Entropy Oxide $(FeCoNiCrMn)_3O_4$ as Anode Towards Superior Lithium Storage Performance. *J. Alloys Compd.* 844, 156158. doi:10.1016/j.jallcom.2020.156158

Wang, J., Cui, Y., Wang, Q., Wang, K., Huang, X., Stenzel, D., et al. (2020b). Lithium Containing Layered High Entropy Oxide Structures. *Sci. Rep.* 10 (1), 1–13. doi:10.1038/s41598-020-75134-1

Wang, J., Stenzel, D., Azmi, R., Najib, S., Wang, K., Jeong, J., et al. (2020c). Spinel to Rock-Salt Transformation in High Entropy Oxides with Li Incorporation. *Electrochem* 1 (1), 60–74. doi:10.3390/electrochem1010007

Wang, K., Nishio, K., Horiba, K., Kitamura, M., Edamura, K., Imazeki, D., et al. (2022a). Synthesis of High-Entropy Layered Oxide Epitaxial Thin Films: $LiCr_{1/}$

$_6Mn_{1/6}Fe_{1/6}Co_{1/6}Ni_{1/6}Cu_{1/6}O_2$. *Cryst. Growth & Des.* 22 (2), 1116–1122. doi:10.1021/acs.cgd.1c01076

Wang, Q., Sarkar, A., Li, Z., Lu, Y., Velasco, L., Bhattacharya, S. S., et al. (2019a). High Entropy Oxides as Anode Material for Li-Ion Battery Applications: A Practical Approach. *Electrochem. Commun.* 100 (January), 121–125. doi:10.1016/j.elecom.2019.02.001

Wang, Q., Sarkar, A., Wang, D., Velasco, L., Azmi, R., Bhattacharya, S. S., et al. (2019b). Multi-Anionic and -Cationic Compounds: New High Entropy Materials for Advanced Li-Ion Batteries. *Energy Environ. Sci.* 12 (8), 2433–2442. doi:10.1039/c9ee00368a

Wang, Q., Velasco, L., Breitung, B., and Presser, V. (2021a). High-Entropy Energy Materials in the Age of Big Data: A Critical Guide to Next-Generation Synthesis and Applications. *Adv. Energy Mater.* 11 (47), 2102355. doi:10.1002/aenm.202102355

Wang, S.-Y., Chen, T.-Y., Kuo, C.-H., Lin, C.-C., Huang, S.-C., Lin, M.-H., et al. (2021b). Operando Synchrotron Transmission X-Ray Microscopy Study on (Mg, Co, Ni, Cu, Zn)O High-Entropy Oxide Anodes for Lithium-Ion Batteries. *Mater. Chem. Phys.* 274 (August), 125105. doi:10.1016/j.matchemphys.2021.125105

Wang, X., Tang, S., Guo, W., Fu, Y., and Manthiram, A. (2021c). Advances in Multimetallic Alloy-Based Anodes for Alkali-Ion and Alkali-Metal Batteries. *Mater. Today* 50 (November), 259–275. doi:10.1016/j.mattod.2021.05.001

Wang, Z., Ge, H., Liu, S., Li, G., and Gao, X. (2022b). High-Entropy Alloys to Activate the Sulfur Cathode for Lithium-Sulfur Batteries. *Energy & Environ. Mater.*, 0–2. doi:10.1002/eem2.12358

Widom, M. (2018). Modeling the Structure and Thermodynamics of High-Entropy Alloys. *J. Mat. Res.* 33 (19), 2881–2898. doi:10.1557/jmr.2018.222

Witte, R., Sarkar, A., Kruk, R., Eggert, B., Brand, R. A., Wende, H., et al. (2019). High-Entropy Oxides: An Emerging Prospect for Magnetic Rare-Earth Transition Metal Perovskites. *Phys. Rev. Mater.* 3 (3), 1–8. doi:10.1103/PhysRevMaterials.3.034406

Witte, R., Sarkar, A., Velasco, L., Kruk, R., Brand, R. A., Eggert, B., et al. (2020). Magnetic Properties of Rare-Earth and Transition Metal Based Perovskite Type High Entropy Oxides. *J. Appl. Phys.* 127 (18), 185109–185110. doi:10.1063/5.0004125

Wu, B., Hou, G., Kovalska, E., Mazanek, V., Marvan, P., Liao, L., et al. (2022). High-Entropy NASICON Phosphates ($Na_3M_2(PO_4)_3$ and $NaMPO_4$Ox, M = Ti, V, Mn, Cr, and Zr) for Sodium Electrochemistry. *Inorg. Chem.* 61 (9), 4092–4101. doi:10.1021/acs.inorgchem.1c03861

Xiang, H.-Z., Xie, H.-X., Chen, Y.-X., Zhang, H., Mao, A., and Zheng, C.-H. (2021b). Porous Spinel-Type $(Al_{0.2}CoCrFeMnNi)_{0.58}O_{4-\delta}$ High-Entropy Oxide as a Novel High-Performance Anode Material for Lithium-Ion Batteries. *J. Mater Sci.* 56 (13), 8127–8142. doi:10.1007/s10853-021-05805-5

Xiang, H., Xing, Y., Dai, F.-z., Wang, H., Su, L., Miao, L., et al. (2021a). High-Entropy Ceramics: Present Status, Challenges, and a Look Forward. *J. Adv. Ceram.* 10 (3), 385–441. doi:10.1007/s40145-021-0477-y

Xiao, B., Wu, G., Wang, T., Wei, Z., Sui, Y., Shen, B., et al. (2021). High Entropy Oxides $(FeNiCrMnX)_3O_4$ (X=Zn, Mg) as Anode Materials for Lithium Ion Batteries. *Ceram. Int.* 47 (24), 33972–33977. doi:10.1016/j.ceramint.2021.08.303

Xiao, B., Wu, G., Wang, T., Wei, Z., Sui, Y., Shen, B., et al. (2022). High-Entropy Oxides as Advanced Anode Materials for Long-Life Lithium-Ion Batteries. *Nano Energy* 95, 106962. doi:10.1016/j.nanoen.2022.106962

Xin, F., Zhou, H., Ji, D., Wang, X., Ding, J., Shi, Y., et al. (2017). Enhanced Electrochemical Performance of Fe-Sn Alloy with Cu Additive as Anode in Lithium-Ion Batteries. *Meet. Abstr.* MA2017-02, 418. doi:10.1149/MA2017-02/4/418

Xu, H., Hu, R., Zhang, Y., Yan, H., Zhu, Q., Shang, J., et al. (2021). Nano High-Entropy Alloy with Strong Affinity Driving Fast Polysulfide Conversion towards Stable Lithium Sulfur Batteries. *Energy Storage Mater.* 43 (August), 212–220. doi:10.1016/j.ensm.2021.09.003

Yan, J., Wang, D., Zhang, X., Li, J., Du, Q., Liu, X., et al. (2020). A High-Entropy Perovskite Titanate Lithium-Ion Battery Anode. *J. Mater Sci.* 55 (16), 6942–6951. doi:10.1007/s10853-020-04482-0

Yang, L., Chen, C., Xiong, S., Zheng, C., Liu, P., Ma, Y., et al. (2021). Multiprincipal Component P2-$Na0.6(Ti_{0.2}Mn_{0.2}Co_{0.2}Ni_{0.2}Ru_{0.2})O_2$ as a High-Rate Cathode for Sodium-Ion Batteries. *Multiprincipal Compon. P2-Na $_{0.6}$ (Ti $_{0.2}$ Mn $_{0.2}$ Co. 0JACS Au* 1 (1), 98–107. doi:10.1021/jacsau.0c00002

Yazhou, K., and Zhiren, Y. (2022). Synthesis, Structure and Electrochemical Properties of Al Doped High Entropy Perovskite $Lix(LiLaCaSrBa)Ti_{1-x}Al_xO_3$. *Ceram. Int.* 48 (4), 5035–5039. doi:10.1016/j.ceramint.2021.11.041

Yeh, J.-W., Chen, S.-K., Lin, S.-J., Gan, J.-Y., Chin, T.-S., Shun, T.-T., et al. (2004). Nanostructured High-Entropy Alloys with Multiple Principal Elements: Novel Alloy Design Concepts and Outcomes. *Adv. Eng. Mat.* 6 (5), 299–303. doi:10.1002/adem.200300567

Yeh, J.-W. (2015). Physical Metallurgy of High-Entropy Alloys. *JOM* 67 (10), 2254–2261. doi:10.1007/s11837-015-1583-5

Zhang, X.-L., Zhang, W.-B., Han, X.-W., Zhang, L., Bao, X., Guo, Y.-W., et al. (2021). Review-Pseudocapacitive Energy Storage Materials from Hägg-Phase Compounds to High-Entropy Ceramics. *J. Electrochem. Soc.* 168 (12), 120521. doi:10.1149/1945-7111/ac3e49

Zhang, Y. (2019). *High-Entropy Materials, Current Science*. Singapore: Springer Singapore. doi:10.1007/978-981-13-8526-1

Zhao, C., Ding, F., Lu, Y., Chen, L., and Hu, Y. S. (2020). High-Entropy Layered Oxide Cathodes for Sodium-Ion Batteries. *Angew. Chem. Int. Ed.* 59 (1), 264–269. doi:10.1002/anie.201912171

Zhao, J., Yang, X., Huang, Y., Du, F., and Zeng, Y. (2021). Entropy Stabilization Effect and Oxygen Vacancies Enabling Spinel Oxide Highly Reversible Lithium-Ion Storage. *ACS Appl. Mat. Interfaces* 13 (49), 58674–58681. doi:10.1021/acsami.1c18362

Conflict of Interest: The authors declare that the research was conducted in the absence of any commercial or financial relationships that could be construed as a potential conflict of interest.

Publisher's Note: All claims expressed in this article are solely those of the authors and do not necessarily represent those of their affiliated organizations, or those of the publisher, the editors and the reviewers. Any product that may be evaluated in this article, or claim that may be made by its manufacturer, is not guaranteed or endorsed by the publisher.